Published in final edited form as:
J Immunol. 2011 February 1; 186(3): 1554–1563. doi:10.4049/jimmunol.1003005.

CD22 is a recycling receptor that can shuttle cargo between the cell surface and endosomal compartments of B cells

Mary K. O'Reilly, **Hua Tian**, and **James C. Paulson**
Department of Chemical Physiology, The Scripps Research Institute, La Jolla, CA, 92037

Abstract

CD22 is a member of the sialic acid-binding Ig-like lectin (Siglec) family that is known to be a regulator of B cell signaling. Its B cell-specific expression makes it an attractive target for immunotoxin-mediated B cell depletion therapy for the treatment of B cell lymphomas and autoimmune diseases. Although CD22 is well documented to be an endocytic receptor, it is believed that following internalization it is targeted for degradation. We show here that CD22 is instead constitutively recycled to the cell surface. We also find that glycan ligand–based cargo is released from CD22 and accumulates intracellularly as CD22 recycles between the cell surface and endosomal compartments. In contrast, antibodies to CD22 do not accumulate, but remain bound to CD22 and recycle to the cell surface. The results have implications for development of agents that target CD22 as an endocytic receptor for delivery of cytotoxic cargo to B cells.

Keywords

CD22; siglec; sialic acid; recycling; endosomes

Introduction

CD22 is a member of a family of sialic acid-binding, immunoglobulin-like lectins (siglecs), that are involved in regulation of cellular activation receptors and cell-cell adhesion (1,2). The primary function of CD22 is to regulate the B cell receptor (BCR) through recruitment of the phosphatase Shp1 upon antigen stimulation (3–6). Contributing to this function in ways that are not completely understood, CD22 also binds to sialoside ligands both on the surface of the same cell, in *cis*, and on other cells, in *trans* (4,7–10). CD22 resides in clathrin-coated pits, undergoing constitutive clathrin-mediated endocytosis (11–13). Upon antigen stimulation, the BCR migrates to detergent-insoluble activation rafts, and from there engages clathrin in a Src-kinase dependent manner (13,14). Although CD22 is excluded from rafts, it ultimately co-localizes with the BCR in fused raft/clathrin domains prior to endocytosis, suggesting that the endocytic function of CD22 is related to its immunomodulatory effects (15–17). In fact, there is evidence that CD22 may regulate the rate of BCR endocytosis (17).

There are six tyrosines within the intracellular domain of CD22, three of which are within immunoreceptor inhibitory tyrosine motifs (ITIMs) that are involved in regulation of its functions. Mutations of both tyrosines in the fifth and sixth ITIM motifs (Y843 and Y863) of CD22 to alanine result in significant reduction in endocytosis of anti-CD22 antibody (αCD22) (11). Mutating one or the other of these tyrosine residues had only minor effects,

Corresponding author: James C. Paulson, Address: 10550 North Torrey Pines Road, MEM L71, La Jolla, CA, 92037, jpaulson@scripps.edu Phone: 1-858-784-9634 FAX: 1-858-784-9690.

consistent with the ability of either one of these motifs to bind the adaptor protein AP50. Another report suggested that tyrosine motifs can be removed without a major impact on uptake of αCD22. However, removal of the cytoplasmic domain abolished endocytosis, and two glutamine residues in a membrane proximal motif were shown to be crucial determinants (18).

Although endocytosed αCD22 colocalizes with the transferrin receptor in recycling compartments (12), the existing model holds that CD22 is degraded following endocytosis, and not recycled back to the cell surface (19). Although the amount of αCD22 internalized by the cell can be up to 2–3 times the amount of CD22 on the cell surface, this has been attributed to αCD22-induced release of intracellular pools of CD22 to the cell surface (20).

As an alternative to using antibodies, we have employed multivalent glycan ligands of CD22 to study the mechanism of endocytosis, and the utility of glycan ligand-based platforms to deliver therapeutic cargo to B cells (21–24). While endocytosis of ligand-bearing nanoparticles has been demonstrated (12,21,22), little is known about the subsequent fate of CD22 or its cargo. We recently reported one such platform, which employs anti-NP IgM (αNP) as a decavalent scaffold to present a heterobifunctional CD22 ligand, ^{BPC}NeuAc-NP, comprising a high-affinity CD22 ligand coupled to the hapten, nitrophenol (NP).(24) In effect, αNP and ^{BPC}NeuAc-NP assemble to display the high-affinity CD22 ligand in a multivalent fashion that competes with *cis* ligands and achieves stable binding to CD22 on the native B cell surface. When using this system to examine endocytosis, we observed a dramatic accumulation of the αNP complex inside the cell. These observations led us to the discovery that CD22 is a recycling receptor, and that the glycan ligand is released at the low pH of endosomes. This behavior accounts for the accumulation of ligand-based cargo in the cell as CD22 cycles between the cell surface and intracellular compartments. In contrast, while αCD22 was efficiently endocytosed, it did not accumulate due to lack of release at low pH, instead recycling to the cell surface with CD22.

Because of its B cell-restricted expression and endocytic function, targeting of immunotoxins to CD22 for the treatment of B cell lymphoma and autoimmune diseases is being actively investigated in clinical trials.(22,25–31) We have recently shown that doxorubicin-loaded liposomes targeted to B cells with glycan ligands of CD22 are also effective in prolonging life in a murine model of B cell lymphoma (21). The results presented here suggest that the efficacy of the ligand-targeting approach may be facilitated by the ability of CD22 to recycle and accumulate ligand-decorated cargo intracellularly.

Materials and Methods

Antibodies and reagents

Anti-NP IgM (αNP) was produced from the B1-8 hybridoma, purified by affinity chromatography, and labeled with Alexafluor488 as described previously. (24) ^{BPA}Neu5Gcα2,6Galβ1,4GlcNAcβ-SpNH-PAA-Biotin (^{BPA}NeuGc-PAA) was prepared as described previously (22). RFB4 αCD22 was obtained from Abcam. Streptavidin-conjugated agarose beads were purchased from Thermo. Rabbit polyclonal H-221 αCD22 was purchased from Santa Cruz Biotechnology, Inc and used for western blotting. Rabbit αV5 was purchased from Sigma-Aldrich and used for western blotting. ReliaBlot HRP-anti-rabbit was used for secondary detection of western blots. Myg13 αCD22 was purchased from Santa Cruz Biotechnology, Inc. and used as an unlabeled primary antibody for flow cytometry with FITC-labeled anti-mouse IgG (Jackson Immunoresearch, 115-096-072) for detection. FITC-labeled anti-mouse IgG+IgM (Jackson Immunoresearch, 115-096-068), FITC-labeled mouse IgG_1 (BD, 349041), and FITC-labeled BL-CAM anti-CD22 (BD, 555424) were also used for flow cytometry. Streptavidin-conjugated magnetic beads were

purchased from Invitrogen. HBSS/B is Hank's Buffered Saline Solution containing 5 mg/mL bovine serum albumin.

cDNA constructs

The cDNA encoding murine CD22.2 was a generous gift from Dr. Edward A. Clark (Primate Center, University of Washington, Seattle, WA).(5) To generate specific CD22 mutants, the GeneTailor Site-Directed Mutagenesis System from Invitrogen (Carlsbad, CA) was used, as directed by the manufacturer, to introduce changes into the CD22 cDNA within the pcDNA3.1 vector (Invitrogen). The intracellular membrane distal motifs containing Y843 and Y863 were mutagenized either singly or in tandem to change the tyrosine residues to alanine, phenylalanine, or aspartate. The intracellular membrane proximal motifs containing R737, S738, Q739 and R737/Q739 were mutagenized to alanine. The mutations were confirmed by sequencing (data not shown).

Mouse and cell lines

Burkitt's human lymphoma BJAB cells (32) were maintained in RPMI containing 10% heat-inactivated fetal bovine serum (BSA) and 50 μM 2-mercaptoethanol (2-ME). Reh cells were purchased from ATCC. Daudi and Reh cells were maintained in in RPMI containing 10% FBS. CHO cells were maintained in 1:1 F12:DMEM containing 10% FBS and either zeocin for wild-type cells or hygromycin as a selection marker for CHO cells stably transfected with a plasmid encoding full-length hCD22(12). The mCD22−/− J2-44 B cell line (33) was kindly provided by Dr. Henry H. Wortis (Tufts University School of Medicine, Boston, MA). The cells were maintained in RPMI 1640 media (Invitrogen) supplemented with 10% FBS, 2 mM glutamine, 100 U/ml penicillin, 100 μg/ml streptomycin sulfate, 0.1 mM nonessential amino acids, 20 mM HEPES, and 50 μM 2-ME (SIGMA). For transfection, the cDNA mutants were subcloned into pQCXIP Retroviral Vector (Clontech, Mountain View, CA). Retrovirus was produced through introducing CMV/MSV/mCD22/IRES/Pur^r and ecotropic packaging constructs into 293 cells (Clontech) by calcium phosphate transfection (Invitrogen). To infect J2-44 cells, 1 ml of retrovirus supernatant was used by spinoculation (2500 × g, 1 h, 25°C) with the presence of 1:1000 lipofectamine (Invitrogen). To generate stable expressing cell lines, 1 μg/ml puromycin was used to select the positive clones. Transfected mCD22/J2-44 cell lines were maintained in complete culture media with 0.5 μg/ml puromycine. C57BL/6J mice were obtained from TSRI in-house breeding program. All mice used in this study were between 6–12 weeks of age and housed in a specific pathogen-free facility according to TSRI IACUC guidelines. After obtaining single-cell suspensions of splenocytes, RBCs were lysed by incubation in 0.15M NH_4Cl, 10mM $KHCO_3$, and 0.1 mM EDTA (pH7.2) for 5 minutes followed by washing with HBSS/B.

Flow cytometry binding and internalization assay—For cargo internalization following pre-binding at 4 °C, 100-μL aliquots of BJAB cells (2×10^6/mL) were incubated with 2 μg Alexa488-labeled αNP and 2 μM NP or ^{BPC}NeuAc-NP ligand in RPMI/10%FBS/50 μM 2-ME media at 4° C for 1.5 hr. Cells were then washed and resuspended in media containing 100 nM ligand (2×10^6/mL). Ligand was added to a concentration of 2 μM to maintain the complex, and cells were warmed to 37 °C to enable internalization. For continuous internalization without pre-binding, αNP and NP or ^{BPC}NeuAc-NP were added to cells as above but were immediately warmed to 37 °C. Following internalization for the indicated times, cells were pelleted and either washed with HBSS/B (pH 7) for the measurement of total αNP (neutral wash), or resuspended in 40 μL-aliquots of 0.133 M citric acid, 0.0666 M sodium carbonate, pH 3.3 to 5×10^6/mL and incubated at 25 °C for 4 min (acid-wash). All cells were washed with HBSS/B and analyzed by flow cytometry (FACSCalibur, BECTON DICKINSON) and CellQuest software. The same protocol was

carried out to test αCD22 binding. 10-μL aliquots of either FITC-labeled mouse IgG_1 or FITC-labeled mouse αCD22 (BL-CAM) were added instead of glycan-based cargo.

Mutant CD22 internalization assays were performed by using J2-44 mouse B cells that had been transfected with either the wild-type or a mutant form of murine CD22. Comparable expression levels of CD22 on J2-44 cell lines was assessed using immunofluorescence staining with flow cytometry(data not shown). 1×10^6 cells were incubated with 5 μg/mL anti-CD22-PE antibody (SouthernBiotech, Birmingham, AL) on ice for 45 min, washed with 1 mL of ice-cold HBSS/B or left in solution with antibody, and then incubated at 37°C or on ice for 60 min. Following incubation, cells were washed with RPMI 1640 at either pH 2.15 or neutral pH. After a final wash with 1 mL of HBSS/B, the cells were analyzed by flow cytometry (FACSCalibur, BECTON DICKINSON) and Flowjo software (Treestar).

To measure binding under hypertonic conditions, BJAB cells (2×10^6/mL) were incubated for 15 minutes at 37 °C in alphaMEM/10% FBS containing 0.45 M sucrose. Cells were washed twice at 4 °C and resuspended to 2×10^6/mL, all with the same media. Alexa488-labeled αNP (2 μg) and 2 μM NP or ^{BPC}NeuAc-NP were added to 100-μL aliquots of cells and incubated at 4 °C or 37 °C for 1.5 hours. Following incubation, cells were washed with 200-μL aliquots of HBSS/B containing 100 nM ligand and then analyzed by flow cytometry. For inhibition of subsequent intracellular trafficking, cells were pre-incubated at 37 °C for 45 minutes in media containing 0.5 μM Bafilomycin A.

CD22 internalization assay with polyacrylamide glycan probe in primary murine B cells

To analyze mCD22 internalization, 10^6 mouse spleen cells were incubated with 0.125 μg of the biotinylated polyacrylamide probe, ^{BPA}NeuGc-PAA, in a total volume of 100μL HBSS/B on ice for 2 hours. Cells were either washed with 1mL HBSS/B, or left in the presence of excess unbound probe, and then incubated with 0.25 μg streptavidin-PE (eBioscience) on ice for 45 minutes. Following incubation, cells that had been washed were washed again with 1 mL HBSS/B, and cells that had not been washed were left with unbound probe in solution. Cells were warmed up to 37 °C or kept on ice for 1 hour. Following incubation, cells were washed with 400 μl of RPMI 1640 (pH2.5) or normal RPMI 1640, followed by two washes of 1mL HBSS/B. Finally, B cells were stained with 0.25 μg of PerCP-Cy5.5 anti-B220 (Biolegend) in a volume of 100 μL on ice for 45 minutes. All flow cytometric data were acquired on FACSCalibur (BECTON DICKINSON) and analyzed using Flowjo program (Treestar).

Fluorescence detection of recycled CD22-bound αCD22

Aliquots of 2×10^5 BJAB cells in 100 μL DPBS/5%FBS were incubated with 2 μg of unlabeled αCD22 (Myg13), isotype control mouse IgG_1, or αNP +/− ^{BPC}NeuAc-NP (2 μM) for 60 minutes at 37 °C. Cells were then washed with neutral DPBS/5%FBS at 4 °C, or acid-washed in 40 μL 0.133 M citric acid, 0.0666 M sodium carbonate, pH 3.3 for 4 minutes at 25 °C. Acid-washed cells were neutralized by adding 20X volume of DPBS/5%FBS, pelleted, and then acid-washed a second time. Pelleted, acid-washed cells were resuspended in 100 μL RPMI1640/10%FBS/2μM 2-ME and either kept on ice or warmed to 37 °C for 30 minutes. Both 4 °C and 37 °C incubated cells were either washed with DPBS/5%FBS or acid-washed once as above. After a final wash with DPBS/5%FBS, cells treated with αCD22 or isotype control were stained with a 1:100 dilution of anti-mouse IgG (FITC), while cells treated with αNP were stained with a 1:100 dilution of anti-mouse IgG+IgM (FITC), for 30 minutes on ice. Cells were washed twice with cold HBSS/B and analyzed by flow cytometry.

Sensitivity of antibody and ligand binding to low pH

Protein A-coated magnetic beads bound to CD22-Fc chimera were incubated with 2 μg isotype control mouse IgG (FITC), 2 μg αCD22 (FITC), 2 μg αNP (Alexa488) alone, or 2 μg αNP with 2 μM ^{BPC}NeuAc-NP in 100 μL phosphate/citrate buffer containing 5 mg/mL BSA, at pH 5, 6, or 7 for 3 hours at 37 °C. Beads were then washed twice with 0.2-mL aliquots of HBSS/B. For ^{BPC}NeuAc-NP containing samples, 100 nM ligand was included in the wash buffer. Beads were then analyzed by flow cytometry.

Endocytosis assay—Endocytosis assays were carried out using published procedures.(34,35) Briefly, BJAB or Daudi cells were harvested and resuspended in 0.5 mL ice-cold DPBS to 2×10^7/mL, and incubated with 2 mg/mL sulfoNHS-SS-biotin (Thermo) at 4 °C for 1 hour with end-over-end rotation. Cells were pelleted and washed twice with 1-mL aliquots of DPBS containing 5% FBS and 25 mM lysine, then once containing only DPBS/5% FBS. All steps were carried out at 4°C unless otherwise indicated. Internalization was induced by incubation at 37 °C in a water bath. Cells were then pelleted and treated three times with 1-mL aliquots of 100 mM sodium 2-mercaptoethanesulfonate (MESNa) in 50 mM Tris-Cl, 100 mM NaCl, pH 8.5, with a 10-minute incubation between each exhange. Control cells were washed with this buffer in the absense of MESNa. Cells were then washed twice with 1-mL aliquots of DPBS containing 5 mg/mL iodoacetimide to quench residual MESNa, once with DPBS, and finally lysed by resuspending pellets in 1-mL aliquots of 50 mM Tris-Cl, 150 mM NaCl, 1% Triton X-100, pH 7.4 containing protease inhibitors (Calbiochem cocktail III) for 30 minutes. After pelleting cell debris, the supernatant was transferred to Streptavidin agarose beads (25 μL slurry washed with lysis buffer) and incubated overnight with end-over-end rotation. Streptavidin beads were then washed five times with lysis buffer before heating to 70 °C for 5 min in reducing loading dye and analyzing by 10% Bis-Tris SDS-PAGE and western blotting. H221 (αCD22) was used for detection of CD22 from B cell lines, while αV5 was used for detection of CD22 and Siglec-F transfectants in CHO cells.

Recycling assay with double MESNa treatment

Biotinylation was carried out as in the endocytosis assay. Cells were then pelleted, resuspended in 1-mL aliquots of DPBS/5%FBS/25mM lysine, and incubated at 4 °C with end-over-end rotation for 30 minutes. Cells were then pelleted, resuspended in 1-mL aliquots of DPBS/5%FBS, and incubated at 37 °C for 30 minutes. After returning to 4 °C, cells were pelleted and resuspended in 1-mL aliquots of 50 mM Tris-Cl, pH 8.5, 100 mM NaCl either with or without 50–100 mM MESNa. Following 30 minutes of end-over-end rotation at 4 °C, cells were pelleted and resuspended in DPBS containing 5 mg/mL iodoacetimide for MESNa-treated samples, then incubated for 15 minutes with end-over-end rotation at 4 °C. Cells were pelleted and resuspended in 1-mL aliquots of DPBS/5%FBS, then warmed to 37 °C for the indicated periods of time for recycling. After returning cells to 4 °C, samples were treated with MESNa (or mock treated) and quenched with iodoacetimide as above. Cells were then lysed and biotinylated proteins captured with streptavidin-agarose as described for the internalization assay.

Recycling assay with magnetic bead capture—To measure recycling, the endocytosis assay was performed with the following modifications. Following biotinylation and washing, cells were warmed to 37 °C in a water bath for 30 minutes to allow internalization to reach equilibrium. Following MESNa treatment and iodoacetimide washing, a second 37 °C incubation step was added to allow externalization of internalized biotinylated proteins. To capture externalized proteins, 100 μL of magnetic streptavidin beads (Invitrogen, Dynal M-280) were incubated with cells in DPBS/5% FBS in a total volume of 500 μL. Beads were first washed and resuspended in DPBS/5% FBS to the

original density. Incubation of beads with cells proceeded for 1 hour on ice with occasional mixing, then 8.2 pmol of free biotin was added from an aqueous solution to quench remaining binding sites and the incubation continued for 30 minutes. Samples were pelleted and resuspended in lysis buffer containing protease inhibitors and 1 μg/mL free biotin. Lysis was allowed to proceed for 30 minutes, then samples were exposed to a magnet to isolate the beads, which were subsequently washed three times with lysis buffer, five times with 1 % SDS, and once more with lysis buffer (1 mL/wash). After heating the beads for 5 minutes at 70 °C in reducing loading buffer, proteins were separated by SDS-PAGE and analyzed by western blotting as described for endocytosis.

Release of CD22 from intracellular compartments—BJAB or Reh cells (1×10^6) were incubated for 1 hour at 37 °C in 1 mL RPMI/10% FBS/50 μM 2-ME alone (control), or with either 40 μg αNP (plus or minus 2 μM ^{BPC}NeuAc-NP), 8 μg murine IgG isotype control, or 8 μg RFB4 αCD22. After washing twice with cold DPBS at 4 °C and resuspending in 0.5 mL cold DPBS, cell surface proteins were labeled with an amine reactive biotin reagent (6 mg/mL) for 1.5 hours at 4 °C. Cells were washed three times with 25 mM lysine in DPBS/5% FBS (1 mL/wash) at 4 °C, incubated in lysis buffer (250 μL/sample) for 30 minutes, and then biotin-tagged surface proteins were isolated using 25-μL aliquots of streptavidin-agarose beads. Immunoprecipitation proceeded overnight at 4 °C with end-over-end rotation, and then beads were centrifuged at the highest speed for 5 minutes at 4 °C. Supernatant was collected and saved as intracellular CD22, since it was protected from biotinylation. Beads were washed five times with lysis buffer (1 mL/wash) and then, in order to normalize volumes of the supernatant and the biotinylated proteins, beads were resuspended in 308 μL of reducing loading buffer before heating to 70 °C for 10 minutes. Supernatants were analyzed by SDS-PAGE and western blotting as described above.

Results

Internalization and accumulation of CD22 ligand-targeted cargo, but not αCD22 in B cells

CD22 endocytosis was first investigated by a flow cytometry assay monitoring uptake of fluorescently labeled αCD22 or ligand-targeted cargo by B cells. The ligand-targeted cargo is anti-nitrophenol IgM (αNP), a multivalent scaffold for the heterobifunctional CD22 ligand, ^{BPC}NeuAc-NP that assembles as a complex with CD22 on B cells (24). Through direct conjugation of αNP with AlexaFluor 488, ^{BPC}NeuAc-NP-mediated uptake of αNP-CD22 complexes at 37 °C could be monitored using flow cytometry. To assess the kinetics of ligand endocytosis, complex formation was allowed to proceed at 4 °C for 60 minutes, after which cells were washed to remove unbound ligand and then warmed to 37 °C. Total cell surface-bound plus internalized αNP was measured by the total cellular fluorescence, while internalized ligand was detected after a brief acid-wash (Fig. 1A, Pre-Bind/Wash). In order to assess cargo uptake in a manner more closely resembling physiological conditions, ligand and αNP were added to cells at 37 °C, and binding and endocytosis were allowed to proceed continuously. Under these conditions, the amount of αNP accumulated within the cell was an order of magnitude greater than the amount that associated with the cells at 4°C (Fig. 1A, Continuous). Moreover, even after 5 minutes, the majority of the αNP is inside the cell, and the amount on the surface decreases as a fraction of the total over time.

To evaluate whether αCD22 would demonstrate the same time-dependent accumulation inside B cells, a fluorescently-labeled antibody to CD22 was incubated with BJAB cells using both the pre-bind/wash conditions and the continuous conditions as were used with the αNP. In contrast to the 10-fold greater association of αNP with the cells at 37 °C compared to 4 °C, there was less than a 2-fold difference in the amount of αCD22 association at the

two temperatures (Fig. 1B). In contrast to αNP uptake, internalization of αCD22 quickly reached a maximum with less than 50% inside the cell and then remained at that level throughout the course of the experiment. The modest increase in αCD22 association at 37 °C under continuous conditions is consistent with the binding of αCD22 to intracellular pools of CD22 brought to the cell surface as previously suggested (20). Cells pre-bound with αCD22 and then washed exhibit a slow decrease in cell-associated fluorescence upon 37 °C incubation. This phenomenon is not seen with the αNP, and may be related to the fact that a fraction of the antibody is localized on the cell surface throughout the time course of the experiment and may slowly dissociate from CD22.

To demonstrate the generality of this phenomenon we tested an alternative glycan ligand platform for its ability to be endocytosed by primary murine B cells. This ligand comprised a multivalent polyacrylamide polymer with pendant high-affinity ligands for murine CD22, ^{BPA}NeuGc-PAA. As reported earlier, the ^{BPA}NeuGc-PAA probe has been shown to compete with *cis* ligands to achieve stable binding to CD22 on native B cells (22). Like the αNP cargo, ^{BPA}NeuGc-PAA accumulates intracellularly, resulting in a 10-fold higher association with the cell upon continuous binding and internalization at 37 °C (Fig. 2B) relative to washing prior to internalization (Fig. 2A). Thus, the release and intracellular accumulation of ligand-bound cargo is seen with two completely different platforms targeting human and murine CD22.

CD22 antibody is not released intracellulary and recycles to the cell surface

The lack of accumulation of αCD22, and the observation that less than 50% of αCD22 was internalized, suggested that αCD22 may not be released intracellularly, and that both CD22 and αCD22 recycle back to the cell surface following endocytosis. As precedence, recycling of antibody bound to the thyrotropin receptors was observed during investigation of its trafficking to intracellular compartments (36). To test this possibility, unlabeled αCD22 was used with a labeled secondary antibody for detection. Unlabeled αCD22 was bound and internalized by the cells, and the labeled secondary antibody was used to detect only residual cell surface αCD22. Fig. 3A shows αCD22 remaining on the cell surface following 37 °C incubation (thick trace), and its subsequent removal with acid (thin trace). Intracellular αCD22 would not be detected under these conditions. Acid-treated cells were then warmed a second time to 37 °C allowing endocytosed αCD22 to recycle to the cell surface, as detected by the labeled secondary antibody (Fig. 3C, thick trace). Following treatment of the cells a second time with acid, the recycled αCD22 was removed from the cell surface (Fig. 3C thin trace). As a control, reappearance of αCD22 was not observed if the cells were left on ice instead of warming to 37 °C in the second incubation (Fig. 3B). As expected, αNP does not re-appear on the cell surface under the same conditions, in agreement with its observed intracellular accumulation, and an isotype control of αCD22 verifies specificity (Supplemental Fig. 1).

Differential pH sensitivity between antibody and glycan ligand binding to CD22

We next investigated the possibility that αNP accumulation may relate to the ability of CD22 to release ligand-based cargo in endosomes. Accordingly, the pH dependence of antibody or glycan ligand binding to CD22 was determined using Protein A-conjugated magnetic beads coated with CD22-Fc fusion protein. Following incubation of beads with labeled αCD22 or labeled αNP and ^{BPC}NeuAc-NP at 37 °C in pH 5, 6, or 7 buffer for 3 hours, beads were washed and analyzed by flow cytometry. As shown in Fig. 4, αCD22 is similar at all pH values tested, while αNP complexation is attenuated at pH 6, and largely abolished at pH 5. These results suggest that ligand–decorated cargo, but not αCD22, may be released at the reduced pH of intracellular compartments.

Insight into the role of CD22 intracellular motifs in endocytosis

To clarify the role of the cytoplasmic domain in CD22 endocytosis, a panel of mutants of murine CD22 were prepared and used to transfect the CD22-deficient J2-44 murine B cell line (Fig. 5A). Wild-type and mutant cells were incubated with fluorescently-labeled αCD22 at 4 °C for one hour, then either left at 4 °C or warmed to 37 °C for one hour. To measure internalized antibody, cells were washed with a low-pH buffer capable of removing surface-associated antibody. Consistent with the results in Fig. 1, warming the wild-type cells in the presence of antibody leads to a similar proportion of bound to internalized αCD22 (Fig. 5B and C). CD22 mutant Y843F is defective in its ability to internalize αCD22 antibody, although Y863F has less of an effect (Fig. 5B). While the effect of Y863F is modest by itself, the double mutant has a more dramatic effect than Y843F alone, suggesting that Y863 may have a compensatory effect in the Y843F mutant. Alanine and aspartate mutants of these tyrosines were also tested (Supplemental Fig. 2). Fig. 5C addresses the membrane proximal motif in which two glutamine residues in the human sequence were found to be crucial for antibody uptake by CD22(18). Mutation of the corresponding residues in the murine CD22 sequence (R737 and Q739) also attenuates internalization of αCD22 in agreement with the previous study. The single mutants, which were not tested previously, extend the understanding of this motif by revealing a more pronounced effect in the Q739A mutant. With the knowledge that CD22-bound antibodies are recycled back to the cell surface, these results suggest that the mutations in both motifs either block internalization, as suggested previously, or, alternatively, lead to a redistribution of CD22 favoring localization on the cell surface.

Accumulation of αNP occurs by clathrin-dependent endocytosis and requires recycling

Based on evidence that CD22 endocytosis is clathrin-mediated, and that CD22 recycles to the cell surface following endocytosis (Fig. 3B), we used conditions known to perturb clathrin-mediated endocytosis to test the possibility that αNP accumulation results from CD22 shuttling cargo from the cell surface to intracellular compartments. As shown in Fig. 6A, endocytosis and accumulation of αNP was blocked by incubating the cells in hypertonic media containing 0.45 M sucrose, which disrupts the formation of clathrin-coated pits (37). The degree of αNP association is similar to that seen at 4° C, where endocytosis is disabled by low temperature. This result demonstrates that accumulation of αNP at 37 °C is not due to enhanced binding of αNP to CD22 on the cell surface at 37 °C, but requires endocytosis.

To assess the effect of blocking more downstream processes, cells were pre-treated with Bafilomycin A (Baf), a potent proton pump inhibitor that is responsible for vesicular acidification and inhibits recycling of endocytosed receptors (34,35,38,39). Accumulation of αNP was blocked by Baf, consistent with a requirement for acidification of endosomes and recycling of CD22 for accumulation of αNP inside the cell (Fig. 6A). Fig. 6B depicts a graphical representation of the data.

Constitutive endocytosis and recycling of CD22

To determine if CD22 also undergoes constitutive recycling, we employed a reversible biotin-tagging strategy that monitors CD22 directly to detect endocytosis and recycling as illustrated in Fig. 7 (34,35). Specifically, lysines of cell surface proteins are labeled at 4 °C with disulfide-linked biotin using the cell impermeable labeling reagent, sulfoNHS-SS-Biotin (sulfosuccinimidyl 2-(biotinamido)-ethyl-1,3-dithiopropionate (Fig. 7-A). This modification is reversible by treatment with the cell-impermeable reducing agent sodium 2-mercapto-ethanesulfonate (MESNa; Fig. 7-B). At any time, biotinylated CD22 is readily assessed by lysing the cells, capturing biotinylated proteins with streptavidin-agarose beads, and analyzing by SDS gel electrophoresis and Western blotting with an antibody to CD22. Endocytosis can then be detected by warming the cells to 37 °C for various times, and after

cooling again to 4 °C, treating with MESNa to removed cell surface biotin. Thus, biotin only remains on proteins that have been endocytosed (Fig. 7-C). By adding a second warming step following MESNa treatment but prior to lysis, recycling can be monitored either by MESNa removal of the biotin tag from CD22 that has reappeared on the cell surface (Fig. 7-E) or by exposing intact cells to streptavidin beads before lysis to capture only the cell surface biotinylated-CD22 (Fig. 7-F).

A key assumption in this strategy is that the biotin-labeling is stable once internalized. To verify this assumption, the level of biotinylated CD22 isolated from cells was compared at 4 °C and 37 °C. If the biotin disulfide is unstable upon internalization, less CD22 should be isolated with streptavidin beads. However, no decrease in streptavidin-isolated CD22 was observed, even after 90 minutes of 37 °C incubation (Supplemental Fig. 3).

Using this strategy, endocytosis of CD22 was assessed in several cell lines including two B cell lines, and CHO cells expressing CD22 (Fig. 8). In BJAB cells, CD22 endocytosis reaches a maximum around 15 minutes, while in Daudi cells, no further endocytosis is observed beyond 5 minutes. Using this assay, we found that the presence of αNP and ^{BPC}NeuAc-NP does not accelerate the rate of CD22 internalization (Supplemental Fig. 4). Siglec-F, which has a distinct endocytic mechanism from CD22, was included for comparison.

To determine if the biotinylated CD22 subsequently recycles, MESNa-treated cells were warmed to 37 °C for various times then treated with or without MESNa at 4 °C (as illustrated in Fig. 7-C,D,E). As shown for BJAB, Daudi, and Reh cells (Fig. 9A), relative to the total amount of labeled endocytosed CD22 (- MESNa), none is sensitive to MESNa treatment at 0 time. With increasing time at 37 °C, the majority of labeled CD22 becomes re-sensitized, demonstrating recycling to the cell surface.

To assess recycling using an alternative approach with a positive read-out, the second MESNa treatment was not performed. Rather, following the second warming step, magnetic streptavidin beads were added to intact cells prior to cell lysis to capture only biotinylated CD22 that reappeared on the cell surface (e.g. Fig. 7-F). After adding excess biotin to quench remaining biotin binding sites on streptavidin, CD22 was probed by Western blotting. Using BJAB, Daudi, and transfected CHO cells, Fig. 9B shows that biotinylated CD22 re-emerges on the cell surface in a time-dependent manner. Notably, the kinetics of recycling were quite different for the different cell lines examined. Re-emergence of endocytosed Siglec-F is not observed, which is consistent with the demonstration that endocytosed Siglec F moves to lysosomal compartments (12).

Redistribution of CD22 to the cell surface by ligation with αCD22, but not by ligand-based cargo

The distribution of CD22 between the cell surface and intracellular compartments in BJAB and Reh B cell lines was evaluated by biotinylating the cell surface proteins at 4 °C and then separating biotinylated from unlabeled (intracellular) CD22 using streptavidin-coated magnetic beads prior to analysis by Western blotting. This was done following pre-incubation of the cells at 37 °C alone, or with either αCD22 or αNP + ^{BPC}NeuAc-NP. In the absence of either αCD22 or ligand-based cargo, BJAB cells have more CD22 expressed on the surface than in intracellular compartments, while the opposite is the case with Reh cells (Fig. 10). This observation Is consistent with the Reh being derived from a pre-B cell leukemia-derived cell line, and previous studies showing that pre-B cells have an increased proportion of intracellular CD22 (40). As reported by others (20), αCD22 induces redistribution of CD22 to the cell surface in both cell lines, with the effect being particularly evident in Reh cells. In contrast, ligand-based cargo does not produce a significant change in

distribution in either cell line (Fig. 10). To confirm, distribution of CD22 in the presence or absence of ligand was repeated in triplicate, with no significant difference in the ratio of extra- to intracellular CD22 (data not shown). These data also support the conclusion that the intracellular accumulation of glycan ligand-targeted cargo is accounted for by recycling of CD22 and not redistribution of intracellular pools to the cell surface.

Discussion

Here we demonstrate that CD22 is an endocytic receptor that efficiently recycles to the cell surface. The conclusion that CD22 recycles to the cell surface is in contrast to previous reports that had suggested CD22 was not recycled following endocytosis (19,20). In a pivotal early study, Shan and Press used an elegant neuraminidase-shift assay that was similar in concept to the biotin labeling assay used here (19). Cell surface ^{125}I-labeled CD22 subjected to isoelectric focusing revealed numerous bands that were collapsed to less acidic species by treatment with neuraminidase. Endocytosis to intracelluar compartments protected the acidic bands from neuraminidase treatment. However, in a recycling experiment, the endocytosed CD22 exhibited little increased sensitivity to neuraminidase over 60 min, while endocytosed transferrin, used as a control, exhibited slight sensitivity after 30 min, and significant sensitivity by 60 minutes. While it was concluded that CD22 does not recycle, we believe that these results are not inconsistent with our observations. We find that the kinetics for recycling is relatively slow, and varies considerably from cell line to cell line (Fig. 9). Moreover, we have previously documented that the kinetics of CD22 endocytosis are significantly delayed from transferrin endocytosis (12), so it would not be surprising if the kinetics of recycling relative to transferrin were also delayed.

As we observed (Fig. 1B), and a consistent finding of various groups, endocytosis of αCD22 plateaus at a fraction (30–80%) of the total bound (18,19,25). This has been interpreted by some investigators as the result of two pools of cell surface CD22 with distinct internalization kinetics, which may be related to its association with the BCR (15,19). In light of our finding that CD22 is a recycling receptor, we believe that the residual cell surface αCD22 is the result of an equiibrium between the intracellular and cell surface pools of CD22, and that antibody, once bound to CD22, is recycled to the cell surface along with CD22 (Fig. 3B).

The demonstration that CD22 is a recycling receptor provides additional perspective on the importance of regulatory motifs in the cytoplasmic domain that affect CD22 endocytosis. One report demonstrated that tyrosines 843 and 863 of two ITIM motifs are important for antibody-induced endocytosis of CD22, using an assay that monitored loss of CD22 from the cell surface(11). Another study used a different CD22 construct and an assay involving endocytosis of a cytotoxin to demonstrate the importance of a motif with two membrane proximal glutamine residues(18). The experiments reported here compare mutants of these sequences on the same murine CD22 construct expressed in a CD22-deficient B cell line, using the same assay, and demonstrate that both sets of sequences are indeed important in endocytosis of αCD22. For the ITIM motifs, the Y843F mutant and double mutant Y843/863F mutant exhibit over 10-fold reduced endocytosis of αCD22 compared to wild type, while the Y863F mutant show little deficiency (Fig. 5B). For the membrane proximal motif, residues R737 and Q739 in murine CD22 were confirmed to be crucial for endocytosis (Fig. 5C). The previous study did not address the two residues individually. Of these two mutations, we found that Q739A is more deleterious, while the double mutant has an even more severe defect. Based on our finding that antibody is recycled with CD22, it is formally possible that the mutations do not affect endocytosis, but instead affect the distribution of CD22 between the cell surface and intracellular compartments. The fact that

the membrane proximal motifs abrogated cytotoxicity to conjugated saporin(15) provides evidence that this is not the case for those mutants.

Antibody ligation is accompanied by an increase in the ratio of CD22 on the cell surface compared to intracellular pools of CD22 (Fig. 10), as also reported by others (20). We found that the constitutive cell surface CD22 as a fraction of the total differed significantly in BJAB (~60%) and Reh cells (~25%). However, in both cell lines, ligation with RFB4 αCD22 significantly increased the ratio of CD22 on the cell surface to intracellular CD22, which was particularly evident in Reh cells. In contrast, CD22 ligand-based cargo did not confer a change in CD22 distribution. While the mechanism of the altered distribution is not yet completely understood, antibody ligation can influence phosphorylation of ITIM motifs(41), which may in turn alter endocytosis and recycling. However, it is important to note that effects on CD22 endocytosis and distribution may be antibody dependent. Indeed, it has been reported that an αCD22 that blocks the ligand-binding site led to phosphorylation of CD22 and increased B cell proliferation, while non-blocking antibodies did not (41–43). Moreover, ligand-blocking antibodies in mice had *in vivo* effects, including depletion of normal and malignant B cells, that were not seen with non-blocking antibodies (44,45).

In contrast to our results with αCD22, ligand-decorated cargo accumulated in the cell over time, and as a result, the amount of cargo left on the cell surface decreases relative to the total amount in the cell over time, until there is little if any cargo on the surface (Fig. 1A) . Since recycling occurs constitutively, and the rate of endocytosis is not affected by glycan ligands (Supplemental Fig. 4), we believe that ligand-based cargo is carried passively to endosomal compartments once bound to CD22. Our results suggest that the accumulation is a result of release of the ligand-based cargo in the low pH endosomal compartments, freeing up CD22 to return back to the cell surface and shuttle additional cargo into the cell. The accumulation of ligand-based cargo was independent of the ligand platform used (e.g. antibody scaffold or polyacrylamide polymer), and was observed with cell lines and primary cells expressing both human and murine CD22. This conclusion that ligand is reseased in acidic endosomal compartments is supported by the kinetics of the accumulation of CD22 ligand, the pH sensitivity of ligand binding to CD22, and the blocking of the intracellular accumulation of ligand–based cargo by inhibition of intracellular vesicle re-acidification with the proton pump inhibitor, Baf A. Since Baf A treatment is known to inhibit recycling by interfering with the transport of internalized receptors back to the cell surface(34,35,38,39), the dramatic blocking of intracelluar accumulation may be the result of both blocking release of the cargo, and inhibiting recycling.

In several respects, the pH dependent release of ligands by CD22 is reminiscent of the behaviour of other well-known recycling receptors. We had previously documented that CD22 is endocytosed to the same compartment as the transferrin receptor (12), which is known to result in a pH dependent release of iron from transferrin, while transferrin is recycled to the surface of the cells and released at neutral pH (46). Even more analogous is the situation with the asialoglycoprotein receptor, which binds glycoproteins containing galactose-terminated glycans, and releases the glycoprotein in acidic lysosomal compartments (47).

The relevance of CD22 endocytosis and recycling to its *in vivo* function is still somewhat of an enigma. Although other siglecs on immune cells have been implicated in the binding and internalization of sialylated pathogens,(12,48–50) no such function has yet been ascribed to CD22 on B cells. However, its constitutive localization to clathrin-coated pits is relevant to its function in B cell receptor (BCR) signaling. The BCR activation complex moves to clathrin domains within minutes of BCR ligation(15,16), and thereby is brought into

proximity with CD22. Thus, it is possible that the primary effect of CD22 recycling is connected to its function as a regulator of cell signaling.

CD22 has long been viewed as an attractive target for immunotherapy of B cell malignancies due to its restricted expression on B cells, and because it is an endocytic receptor that can be exploited as a trojan horse for delivery of drugs intracellularly (27,51). Several αCD22 constructs in human clinical trials are immunotoxins that rely on the endocytic activity of CD22 to deliver conjugated toxin into the cell. These include CM544, an IgG conjugated to calicheamycin, as well as BL22 and its mutated version HA22, which are conjugated to *Pseudomonas* exotoxin (20,26,28–30,52–62). In the case of BL22, ligation with CD22 correlated with a decrease in intracellular CD22 and stoichiometric association of BL22 with total CD22, suggesting a mobilization of CD22 to the cell surface. These observations are consistent with results obtained with RFB4 αCD22 studied here and further suggest that BL22 is not released, but recycles between the cell surface and endosomal compartments. Because CD22 is a recycling receptor, the efficacy of therapeutic CD22 immunotoxins might be improved by optimization of a cleavable linker between the toxin and antibody (29,63), or by using antibodies that exhibit pH-dependent binding to CD22 and are released in the endosome..

As an alternative approach to targeting lymphoma cells *in vivo* we have demonstrated that doxorubicin-loaded liposomal nanoparticles decorated with CD22 ligands provide prolonged survival in a murine model of B cell lymphoma (21). Like the ligand-targeted platforms examined in this report, the CD22-targeted liposomes accumulate intracellularly in endosomal and lysosomal compartments over time (21). In principle, the release and accumulation of cargo in endosomal compartments as CD22 recycles to the cell surface offers an advantage for the glycan ligand-based targeting approach for cell-directed immunotherapy.

Supplementary Material

Refer to Web version on PubMed Central for supplementary material.

Acknowledgments

We thank Dr. Henry Wortis, Dr. R.B. Corley, and Dr. Michael Pawlita for gifts of the mCD22−/− J2-44 B cell line, anti-NP IgM-producing B1-8 hybridoma, and BJAB B cell lines, respectively. We also thank Dr. Ramya T.N. Chakravarthy, Cory Rillahan, Dr. Christoph Rademacher, Dr. Norihito Kawasaki, and Dr. Kyle Chiang for helpful discussions, and Anna Tran-Crie for assistance in preparation of the manuscript.

This work was funded by NIH grant AI050143. M.K.O. was supported by a postdoctoral fellowship from the American Cancer Society.

Abbreviations

^{BPC}NeuAc	9-Biphenylcarbonyl-*N*-acetylneuraminic acid-α2,6-galactose-β1,4*N*-acetylglucosamine
NP	nitrophenol
MESNa	sodium mercaptoethanesulfonic acid
αNP	anti-nitrophenol IgM
αCD22	anti-CD22 IgG

References

1. Crocker PR, Paulson JC, Varki A. Siglecs and their roles in the immune system. Nat Rev Immunol. 2007; 7:255–266. [PubMed: 17380156]
2. Crocker PR, Redelinghuys P. Siglecs as positive and negative regulators of the immune system. Biochem Soc Trans. 2008; 36:1467–1471. [PubMed: 19021577]
3. Doody GM, Justement LB, Delibrias CC, Matthews RJ, Lin J, Thomas ML, Fearon DT. A role in B cell activation for CD22 and the protein tyrosine phosphatase SHP. Science. 1995; 269:242–244. [PubMed: 7618087]
4. Walker JA, Smith KG. CD22: an inhibitory enigma. Immunology. 2008; 123:314–325. [PubMed: 18067554]
5. Otipoby KL, Draves KE, Clark EA. CD22 regulates B cell receptor-mediated signals via two domains that independently recruit Grb2 and SHP-1. J Biol Chem. 2001; 276:44315–44322. [PubMed: 11551923]
6. Zhu C, Sato M, Yanagisawa T, Fujimoto M, Adachi T, Tsubata T. Novel binding site for Src homology 2-containing protein-tyrosine phosphatase-1 in CD22 activated by B lymphocyte stimulation with antigen. J Biol Chem. 2008; 283:1653–1659. [PubMed: 18024433]
7. Collins BE, Blixt O, DeSieno AR, Bovin N, Marth JD, Paulson JC. Masking of CD22 by cis ligands does not prevent redistribution of CD22 to sites of cell contact. Proc Natl Acad Sci U S A. 2004; 101:6104–6109. [PubMed: 15079087]
8. Han S, Collins BE, Bengtson P, Paulson JC. Homomultimeric complexes of CD22 in B cells revealed by protein-glycan cross-linking. Nat Chem Biol. 2005; 1:93–97. [PubMed: 16408005]
9. Ramya TN, Weerapana E, Liao L, Zeng Y, Tateno H, Yates JR 3rd, Cravatt BF, Paulson JC. In situ trans ligands of CD22 identified by glycan-protein photo-cross-linking enabled proteomics. Mol Cell Proteomics.
10. Razi N, Varki A. Masking and unmasking of the sialic acid-binding lectin activity of CD22 (Siglec-2) on B lymphocytes. Proc Natl Acad Sci U S A. 1998; 95:7469–7474. [PubMed: 9636173]
11. John B, Herrin BR, Raman C, Wang YN, Bobbitt KR, Brody BA, Justement LB. The B cell coreceptor CD22 associates with AP50, a clathrin-coated pit adapter protein, via tyrosine-dependent interaction. J Immunol. 2003; 170:3534–3543. [PubMed: 12646615]
12. Tateno H, Li H, Schur MJ, Bovin N, Crocker PR, Wakarchuk WW, Paulson JC. Distinct endocytic mechanisms of CD22 (Siglec-2) and Siglec-F reflect roles in cell signaling and innate immunity. Mol Cell Biol. 2007; 27:5699–5710. [PubMed: 17562860]
13. Stoddart A, Dykstra ML, Brown BK, Song W, Pierce SK, Brodsky FM. Lipid rafts unite signaling cascades with clathrin to regulate BCR internalization. Immunity. 2002; 17:451–462. [PubMed: 12387739]
14. Stoddart A, Jackson AP, Brodsky FM. Plasticity of B cell receptor internalization upon conditional depletion of clathrin. Mol Biol Cell. 2005; 16:2339–2348. [PubMed: 15716350]
15. Leprince C, Draves KE, Geahlen RL, Ledbetter JA, Clark EA. CD22 associates with the human surface IgM-B-cell antigen receptor complex. Proc Natl Acad Sci U S A. 1993; 90:3236–3240. [PubMed: 8475064]
16. Collins BE, Smith BA, Bengtson P, Paulson JC. Ablation of CD22 in ligand-deficient mice restores B cell receptor signaling. Nat Immunol. 2006; 7:199–206. [PubMed: 16369536]
17. Grewal PK, Boton M, Ramirez K, Collins BE, Saito A, Green RS, Ohtsubo K, Chui D, Marth JD. ST6Gal-I restrains CD22-dependent antigen receptor endocytosis and Shp-1 recruitment in normal and pathogenic immune signaling. Mol Cell Biol. 2006; 26:4970–4981. [PubMed: 16782884]
18. Chan CH, Wang J, French RR, Glennie MJ. Internalization of the lymphocytic surface protein CD22 is controlled by a novel membrane proximal cytoplasmic motif. J Biol Chem. 1998; 273:27809–27815. [PubMed: 9774390]
19. Shan D, Press OW. Constitutive endocytosis and degradation of CD22 by human B cells. J Immunol. 1995; 154:4466–4475. [PubMed: 7722303]

20. Du X, Beers R, Fitzgerald DJ, Pastan I. Differential cellular internalization of anti-CD19 and -CD22 immunotoxins results in different cytotoxic activity. Cancer Res. 2008; 68:6300–6305. [PubMed: 18676854]
21. Chen WC, Completo GC, Sigal DS, Crocker PR, Saven A, Paulson JC. In vivo targeting of B-cell lymphoma with glycan ligands of CD22. Blood. 2010
22. Collins BE, Blixt O, Han S, Duong B, Li H, Nathan JK, Bovin N, Paulson JC. High-affinity ligand probes of CD22 overcome the threshold set by cis ligands to allow for binding, endocytosis, and killing of B cells. J Immunol. 2006; 177:2994–3003. [PubMed: 16920935]
23. Kaltgrad E, O'Reilly MK, Liao L, Han S, Paulson JC, Finn MG. On-virus construction of polyvalent glycan ligands for cell-surface receptors. J Am Chem Soc. 2008; 130:4578–4579. [PubMed: 18341338]
24. O'Reilly MK, Collins BE, Han S, Liao L, Rillahan C, Kitov PI, Bundle DR, Paulson JC. Bifunctional CD22 ligands use multimeric immunoglobulins as protein scaffolds in assembly of immune complexes on B cells. J Am Chem Soc. 2008; 130:7736–7745. [PubMed: 18505252]
25. Press OW, Farr AG, Borroz KI, Anderson SK, Martin PJ. Endocytosis and degradation of monoclonal antibodies targeting human B-cell malignancies. Cancer Res. 1989; 49:4906–4912. [PubMed: 2667754]
26. Castillo J, Winer E, Quesenberry P. Newer monoclonal antibodies for hematological malignancies. Exp Hematol. 2008; 36:755–768. [PubMed: 18565392]
27. O'Reilly MK, Paulson JC. Siglecs as targets for therapy in immune-cell-mediated disease. Trends Pharmacol Sci. 2009; 30:240–248. [PubMed: 19359050]
28. Dijoseph JF, Dougher MM, Armellino DC, Evans DY, Damle NK. Therapeutic potential of CD22-specific antibody-targeted chemotherapy using inotuzumab ozogamicin (CMC-544) for the treatment of acute lymphoblastic leukemia. Leukemia. 2007; 21:2240–2245. [PubMed: 17657218]
29. DiJoseph JF, Dougher MM, Kalyandrug LB, Armellino DC, Boghaert ER, Hamann PR, Moran JK, Damle NK. Antitumor efficacy of a combination of CMC-544 (inotuzumab ozogamicin), a CD22-targeted cytotoxic immunoconjugate of calicheamicin, and rituximab against non-Hodgkin's B-cell lymphoma. Clin Cancer Res. 2006; 12:242–249. [PubMed: 16397048]
30. DiJoseph JF, Popplewell A, Tickle S, Ladyman H, Lawson A, Kunz A, Khandke K, Armellino DC, Boghaert ER, Hamann P, Zinkewich-Peotti K, Stephens S, Weir N, Damle NK. Antibody-targeted chemotherapy of B-cell lymphoma using calicheamicin conjugated to murine or humanized antibody against CD22. Cancer Immunol Immunother. 2005; 54:11–24. [PubMed: 15693135]
31. Sieber T, Schoeler D, Ringel F, Pascu M, Schriever F. Selective internalization of monoclonal antibodies by B-cell chronic lymphocytic leukaemia cells. Br J Haematol. 2003; 121:458–461. [PubMed: 12716368]
32. Keppler OT, Hinderlich S, Langner J, Schwartz-Albiez R, Reutter W, Pawlita M. UDP-GlcNAc 2-epimerase: a regulator of cell surface sialylation. Science. 1999; 284:1372–1376. [PubMed: 10334995]
33. Jin L, McLean PA, Neel BG, Wortis HH. Sialic acid binding domains of CD22 are required for negative regulation of B cell receptor signaling. J Exp Med. 2002; 195:1199–1205. [PubMed: 11994425]
34. Le TL, Yap AS, Stow JL. Recycling of E-cadherin: a potential mechanism for regulating cadherin dynamics. J Cell Biol. 1999; 146:219–232. [PubMed: 10402472]
35. Morimoto S, Nishimura N, Terai T, Manabe S, Yamamoto Y, Shinahara W, Miyake H, Tashiro S, Shimada M, Sasaki T. Rab13 mediates the continuous endocytic recycling of occludin to the cell surface. J Biol Chem. 2005; 280:2220–2228. [PubMed: 15528189]
36. Baratti-Elbaz C, Ghinea N, Lahuna O, Loosfelt H, Pichon C, Milgrom E. Internalization and recycling pathways of the thyrotropin receptor. Mol Endocrinol. 1999; 13:1751–1765. [PubMed: 10517676]
37. Heuser JE, Anderson RG. Hypertonic media inhibit receptor-mediated endocytosis by blocking clathrin-coated pit formation. J Cell Biol. 1989; 108:389–400. [PubMed: 2563728]

38. Johnson LS, Dunn KW, Pytowski B, McGraw TE. Endosome acidification and receptor trafficking: bafilomycin A1 slows receptor externalization by a mechanism involving the receptor's internalization motif. Mol Biol Cell. 1993; 4:1251–1266. [PubMed: 8167408]
39. Presley JF, Mayor S, McGraw TE, Dunn KW, Maxfield FR. Bafilomycin A1 treatment retards transferrin receptor recycling more than bulk membrane recycling. J Biol Chem. 1997; 272:13929–13936. [PubMed: 9153255]
40. Konikova E, Kusenda J, Babusikova O, Glasova M. Human hematopoietic cell lines: a model system for study of minimal residual disease detection technique in acute leukemia. Neoplasma. 1995; 42:227–234. [PubMed: 8552200]
41. Tuscano J, Engel P, Tedder TF, Kehrl JH. Engagement of the adhesion receptor CD22 triggers a potent stimulatory signal for B cells and blocking CD22/CD22L interactions impairs T-cell proliferation. Blood. 1996; 87:4723–4730. [PubMed: 8639842]
42. Tuscano JM, Engel P, Tedder TF, Agarwal A, Kehrl JH. Involvement of p72syk kinase, p53/56lyn kinase and phosphatidyl inositol-3 kinase in signal transduction via the human B lymphocyte antigen CD22. Eur J Immunol. 1996; 26:1246–1252. [PubMed: 8647200]
43. Tuscano JM, Riva A, Toscano SN, Tedder TF, Kehrl JH. CD22 cross-linking generates B-cell antigen receptor-independent signals that activate the JNK/SAPK signaling cascade. Blood. 1999; 94:1382–1392. [PubMed: 10438726]
44. Haas KM, Sen S, Sanford IG, Miller AS, Poe JC, Tedder TF. CD22 ligand binding regulates normal and malignant B lymphocyte survival in vivo. J Immunol. 2006; 177:3063–3073. [PubMed: 16920943]
45. Tuscano JM, O'Donnell RT, Miers LA, Kroger LA, Kukis DL, Lamborn KR, Tedder TF, DeNardo GL. Anti-CD22 ligand-blocking antibody HB22.7 has independent lymphomacidal properties and augments the efficacy of 90Y-DOTA-peptide-Lym-1 in lymphoma xenografts. Blood. 2003; 101:3641–3647. [PubMed: 12511412]
46. Ciechanover A, Schwartz AL, Dautry-Varsat A, Lodish HF. Kinetics of internalization and recycling of transferrin and the transferrin receptor in a human hepatoma cell line. Effect of lysosomotropic agents. J Biol Chem. 1983; 258:9681–9689. [PubMed: 6309781]
47. Ciechanover A, Schwartz AL, Lodish HF. The asialoglycoprotein receptor internalizes and recycles independently of the transferrin and insulin receptors. Cell. 1983; 32:267–275. [PubMed: 6297785]
48. Avril T, Wagner ER, Willison HJ, Crocker PR. Sialic acid-binding immunoglobulin-like lectin 7 mediates selective recognition of sialylated glycans expressed on Campylobacter jejuni lipooligosaccharides. Infect Immun. 2006; 74:4133–4141. [PubMed: 16790787]
49. Carlin AF, Uchiyama S, Chang YC, Lewis AL, Nizet V, Varki A. Molecular mimicry of host sialylated glycans allows a bacterial pathogen to engage neutrophil Siglec-9 and dampen the innate immune response. Blood. 2009; 113:3333–3336. [PubMed: 19196661]
50. Rempel H, Calosing C, Sun B, Pulliam L. Sialoadhesin expressed on IFN-induced monocytes binds HIV-1 and enhances infectivity. PLoS One. 2008; 3:e1967. [PubMed: 18414664]
51. Kreitman RJ, Pastan I. BL22 and lymphoid malignancies. Best Pract Res Clin Haematol. 2006; 19:685–699. [PubMed: 16997177]
52. Bogner C, Dechow T, Ringshausen I, Wagner M, Oelsner M, Lutzny G, Licht T, Peschel C, Pastan I, Kreitman RJ, Decker T. Immunotoxin BL22 induces apoptosis in mantle cell lymphoma (MCL) cells dependent on Bcl-2 expression. Br J Haematol. 148:99–109. [PubMed: 19821820]
53. Wayne AS, Kreitman RJ, Findley HW, Lew G, Delbrook C, Steinberg SM, Stetler-Stevenson M, Fitzgerald DJ, Pastan I. Anti-CD22 immunotoxin RFB4(dsFv)-PE38 (BL22) for CD22-positive hematologic malignancies of childhood: preclinical studies and phase I clinical trial. Clin Cancer Res. 16:1894–1903. [PubMed: 20215554]
54. Keppler-Hafkemeyer A, Kreitman RJ, Pastan I. Apoptosis induced by immunotoxins used in the treatment of hematologic malignancies. Int J Cancer. 2000; 87:86–94. [PubMed: 10861457]
55. Kreitman RJ, Margulies I, Stetler-Stevenson M, Wang QC, FitzGerald DJ, Pastan I. Cytotoxic activity of disulfide-stabilized recombinant immunotoxin RFB4(dsFv)-PE38 (BL22) toward fresh malignant cells from patients with B-cell leukemias. Clin Cancer Res. 2000; 6:1476–1487. [PubMed: 10778980]

56. Kreitman RJ, Wilson WH, Bergeron K, Raggio M, Stetler-Stevenson M, FitzGerald DJ, Pastan I. Efficacy of the anti-CD22 recombinant immunotoxin BL22 in chemotherapy-resistant hairy-cell leukemia. N Engl J Med. 2001; 345:241–247. [PubMed: 11474661]

57. Decker T, Oelsner M, Kreitman RJ, Salvatore G, Wang QC, Pastan I, Peschel C, Licht T. Induction of caspase-dependent programmed cell death in B-cell chronic lymphocytic leukemia by anti-CD22 immunotoxins. Blood. 2004; 103:2718–2726. [PubMed: 14525789]

58. Bang S, Nagata S, Onda M, Kreitman RJ, Pastan I. HA22 (R490A) is a recombinant immunotoxin with increased antitumor activity without an increase in animal toxicity. Clin Cancer Res. 2005; 11:1545–1550. [PubMed: 15746059]

59. Ho M, Kreitman RJ, Onda M, Pastan I. In vitro antibody evolution targeting germline hot spots to increase activity of an anti-CD22 immunotoxin. J Biol Chem. 2005; 280:607–617. [PubMed: 15491997]

60. Kreitman RJ, Squires DR, Stetler-Stevenson M, Noel P, FitzGerald DJ, Wilson WH, Pastan I. Phase I trial of recombinant immunotoxin RFB4(dsFv)-PE38 (BL22) in patients with B-cell malignancies. J Clin Oncol. 2005; 23:6719–6729. [PubMed: 16061911]

61. Onda M, Beers R, Xiang L, Nagata S, Wang QC, Pastan I. An immunotoxin with greatly reduced immunogenicity by identification and removal of B cell epitopes. Proc Natl Acad Sci U S A. 2008; 105:11311–11316. [PubMed: 18678888]

62. Kreitman RJ, Stetler-Stevenson M, Margulies I, Noel P, Fitzgerald DJ, Wilson WH, Pastan I. Phase II trial of recombinant immunotoxin RFB4(dsFv)-PE38 (BL22) in patients with hairy cell leukemia. J Clin Oncol. 2009; 27:2983–2990. [PubMed: 19414673]

63. Polson AG, Calemine-Fenaux J, Chan P, Chang W, Christensen E, Clark S, de Sauvage FJ, Eaton D, Elkins K, Elliott JM, Frantz G, Fuji RN, Gray A, Harden K, Ingle GS, Kljavin NM, Koeppen H, Nelson C, Prabhu S, Raab H, Ross S, Slaga DS, Stephan JP, Scales SJ, Spencer SD, Vandlen R, Wranik B, Yu SF, Zheng B, Ebens A. Antibody-drug conjugates for the treatment of non-Hodgkin's lymphoma: target and linker-drug selection. Cancer Res. 2009; 69:2358–2364. [PubMed: 19258515]

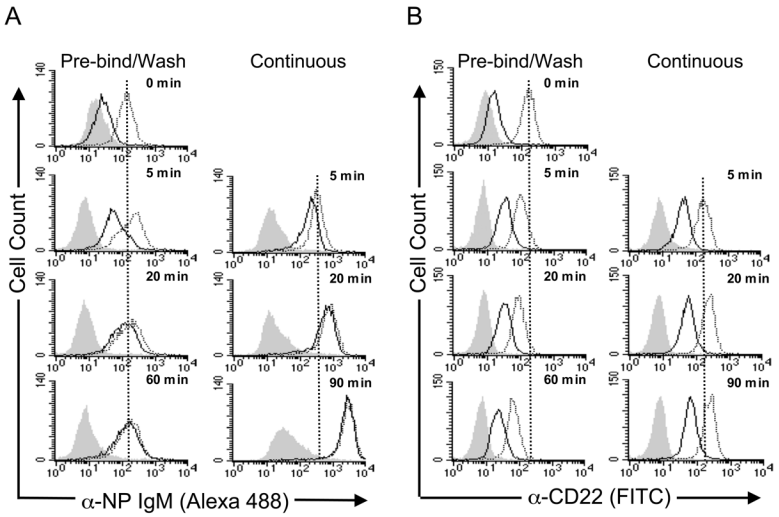

Figure 1. CD22 efficiently internalizes αNP and αCD22 at 37 °C

Native BJAB cells were incubated with (A) αNP +/− ^{BPC}NeuAc-NP, or (B) αCD22/isotype control, under two different sets of conditions. Pre-Bind/Wash: Cells were pre-incubated with αCD22/isotype control, or αNP +/− ^{BPC}NeuAc-NP, at 4° C to allow binding to occur. After washing to remove unbound reagents, cells were warmed to 37 °C to enable internalization. Continuous: αCD22/isotype control, or αNP +/− ^{BPC}NeuAc-NP were added to cells at 37 °C without pre-incubation, allowing binding and internalization to proceed continuously. At the indicated time points, cells were treated with pH 3.3 buffer (solid line) to measure internalized αNP or pH 7 buffer (shaded and dotted) to measure total αNP and read by flow cytometry. Grey filled histograms represent αNP without ^{BPC}NeuAc-NP (A) or isotype control (B). Dotted traces are total antibody binding, and solid traces are internalized antibody.

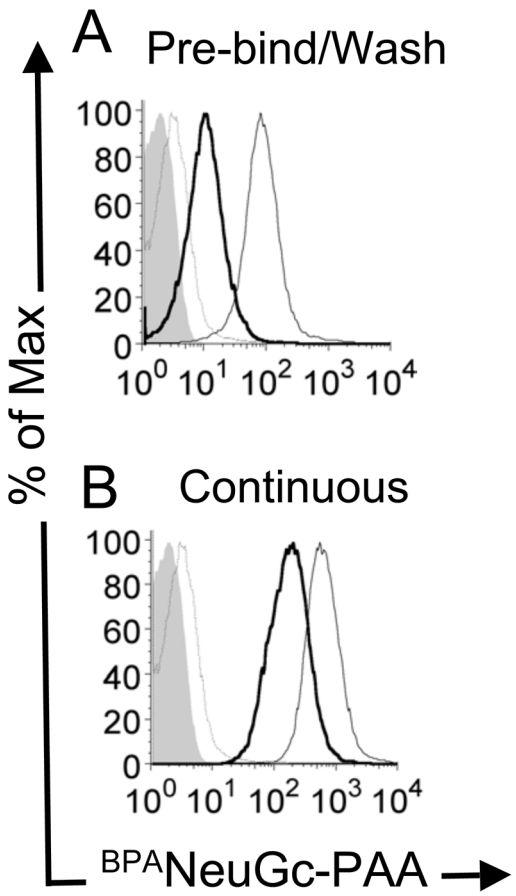

Figure 2. ^{BPA}NeuGc-PAA internalization in mouse primary B cells

Primary murine B cells were incubated with biotinylated ^{BPA}NeuGc-PAA and streptavidin-PE at 4 °C, and either (A) washed to remove unbound ^{BPA}NeuGc-PAA prior to warming to 37 °C; or (B) not washed before warming to 37 °C. Shown is cell-associated ^{BPA}NeuGc-PAA for acid washed cells following the initial 4 °C incubation (*thin grey line*); total cell associated ^{BPA}NeuGc-PAA after warming to 37°C (*thin black line*), and internalized ^{BPA}NeuGc-PAA resistant to an acid wash (*thick black line*). Filled grey trace represents background fluorescence of the cells with no ^{BPA}NeuGc-PAA.

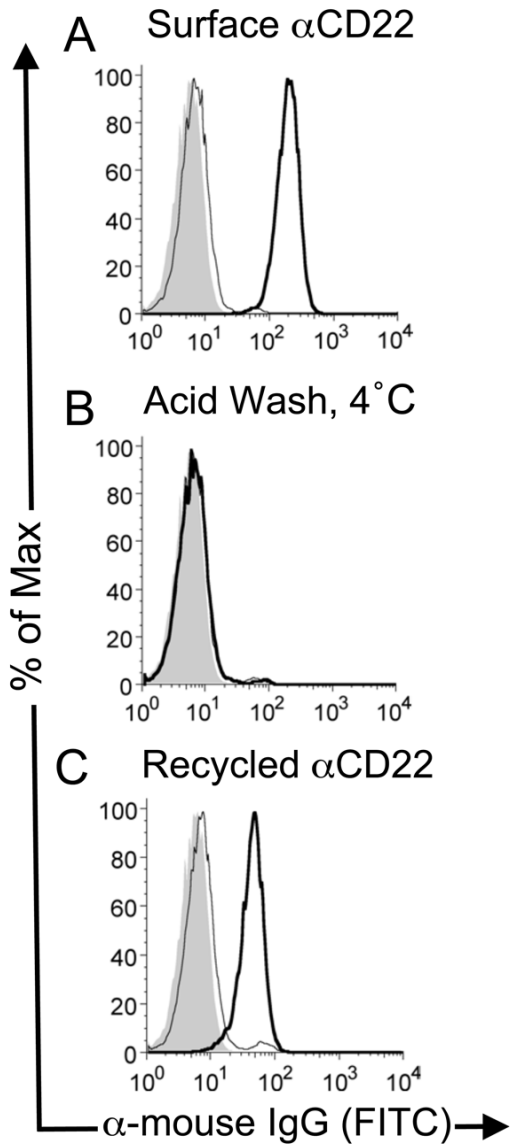

Figure 3. αCD22 recycles back to the cell surface following endocytosis

(A) Unlabeled αCD22 was allowed to bind and internalize in BJAB cells at 37 °C. Cells were then cooled to 4 °C and were stained with a labeled secondary antibody after a neutral wash (*thick line*) or acid wash (*thin line*) to detect residual cell surface bound αCD22. (B) As a control, cells acid-washed cells from panel A were subjected to a further incubation at 4 °C and re-stained with labeled secondary antibody, showing that no αCD22 had returned to the cell surface. (C) Acid-washed cells from the first step were warmed again to 37° C to allow αCD22 to be recycled back to the cell surface. Antibody re-appearing on the surface of the cell is detected by staining the cells with labeled secondary antibody (*thick line*), which is eliminated by stripping with an acid wash (*thin line*).

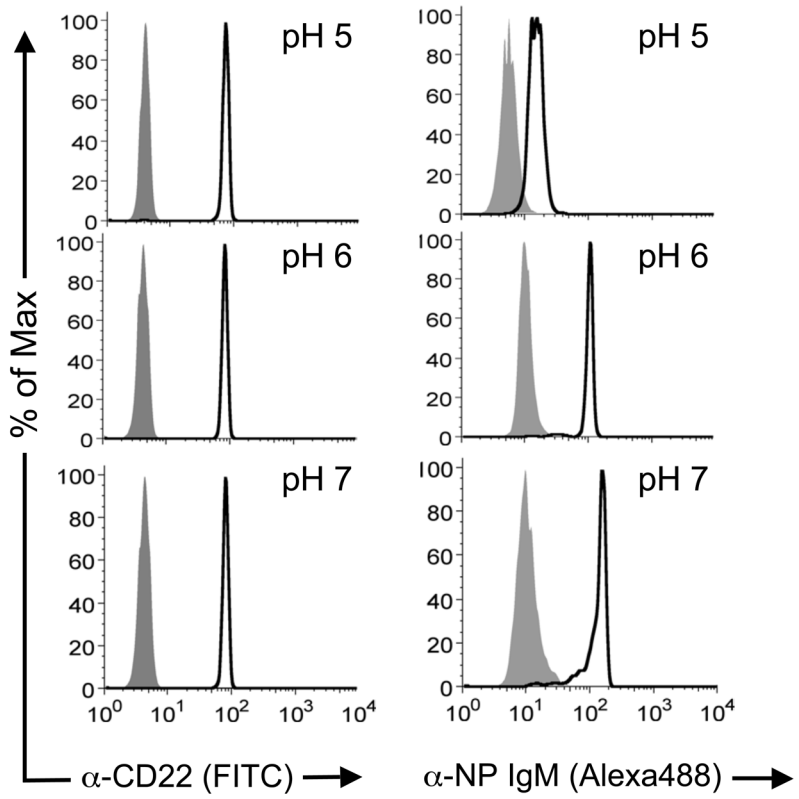

Figure 4. Differential pH dependence for αCD22 binding and ^{BPC}NeuAc-NP mediated αNP binding CD22

CD22-Fc loaded Protein A magnetic beads were incubated with αCD22 or αNP +/– ^{BPC}NeuAc-NP at pH values 5–7 at 37 °C for three hours, then washed and analyzed by flow cytometry. Black traces are αCD22 (left panels) and αNP with ^{BPC}NeuAc-NP (right panel). Grey filled traces are isotype control (left panel) and αNP alone (right panel).

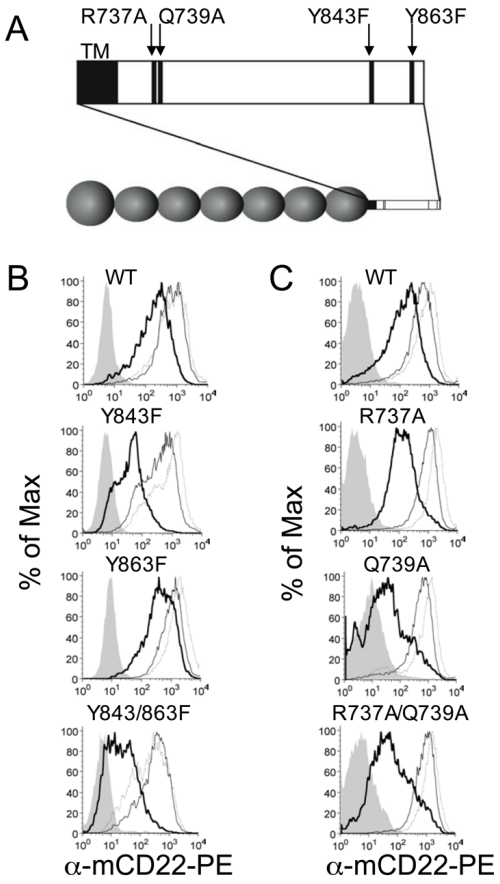

Figure 5. Mutations in the mCD22 cytosolic domain diminish internalization of αCD22

mCD22−/− J2–44 murine B cell lines transfected with wild type and mutant mCD22 were tested for internalization of fluorescently labeled αCD22 antibody: (A) single and double CD22 mutations of Y843F and Y863F; and (B) single and double mutants of R737A and Q739A. Cells were incubated at 4 ° C with antibody and then washed (thin line) or not washed (dotted line) prior to the 37 °C incubation. Cells that were not washed prior to 37° C incubation were also acid-washed following the warming step to reveal internalized antibody (thick line). Cells that were acid-washed following the 4 °C incubation were included as control (filled curve).

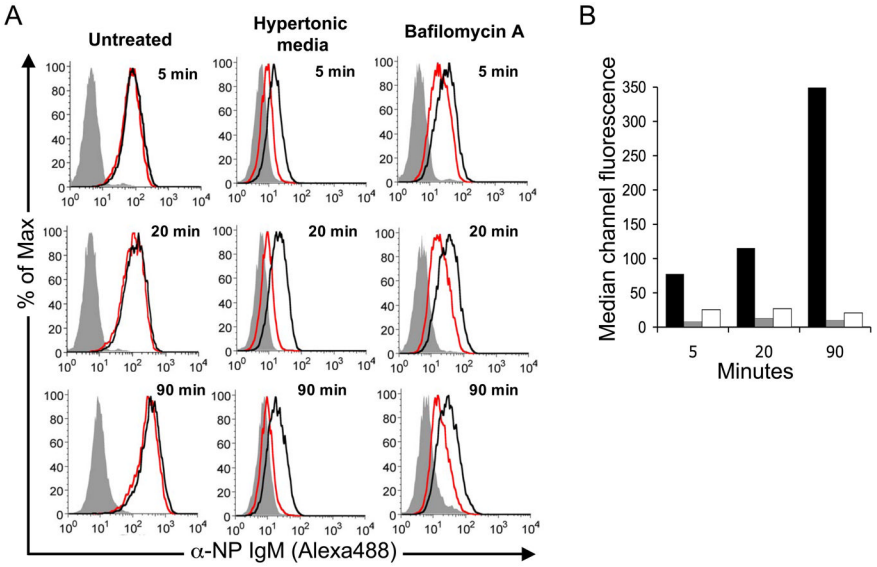

Figure 6. αNP accumulation requires endocytosis and recycling pathways

A. ^{BPC}NeuAc-NP-mediated binding and uptake of αNP (Alexa448) was monitored using BJAB cells in media alone (Untreated), in media containing 0.45 M sucrose to create hypertonicity and block clathrin-dependent endocytosis (Hypertonic Media), or in media containing Bafilomycin A to block recycling by inhibiting re-acidification of intracellular vesicles and trapping internalized CD22 in early endosomes (Bafilomycin A). Analysis was carried out as in Fig. 1, using the conditions for continuous binding and uptake. Filled grey traces are αNP without ^{BPC}NeuAc-NP, black traces are total αNP association, and red traces are internalized αNP. B. Graphical representation of the mean channel fluorescence derived from the histograms in A. Black bars represent untreated, grey bars are cells in hypertonic media, and white bars are Baf A treated cells.

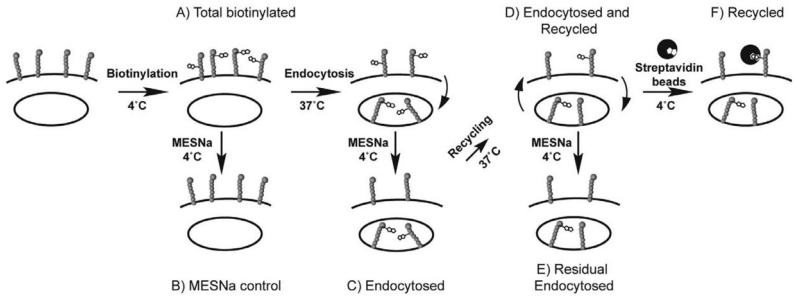

Figure 7. Schematic summary of internalization and recycling assays with biotinylated CD22

Endocytosis Assay: A) Cells are labeled with a cell-impermeable, reversible biotinylating reagent (sulfoNHS-SS-biotin) at 4° C. B) Cells are warmed to 37° C to induce endocytosis. C) At 4° C, cells are treated with the cell-impermeable reducing agent, mercaptoethanesulfonic acid (MESNa), to remove surface biotinylation. Cells can be lysed, immunoprecipitated with streptavidin-agarose, and analyzed by western blotting at this stage to measure internalization. Recycling Assay to detect the return of MESNa-sensitive CD22: D) Cells are warmed a second time to allow return of recycling proteins to the cell surface. E) Cells are treated a second time with MESNa to remove biotin from recycled proteins, then are lysed, immunoprecipitated with streptavidin-agarose beads, and analyzed by western blotting. Loss of signal following second MESNa treatment indicates recycling. Recycling Assay Using Cell Surface Capture: F) After the second warming step, instead of a second MESNa treatment, cell surface biotinylated proteins (recycled) are isolated by streptavidin-coated magnetic beads at 4 °C. After quenching excess binding sites with biotin, cells are lysed, and bead-bound proteins are analyzed by western blotting. Recovery of the signal indicates recycling.

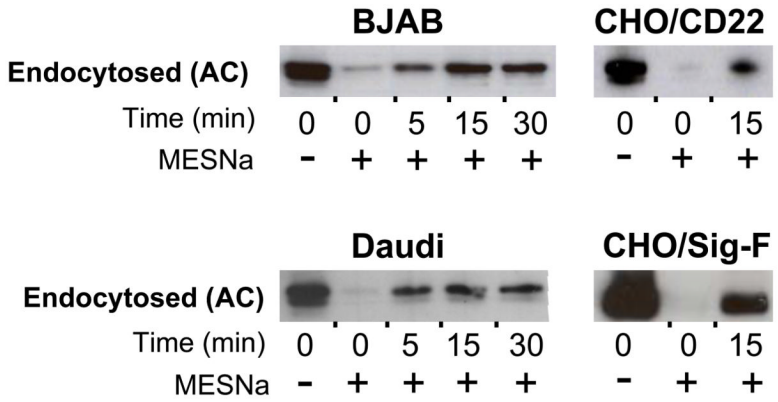

Figure 8. Endocytosis of biotinylated CD22

Shown are endocytosis experiments measuring increasing amounts of MESNa-resistant biotin signal. Steps A-C from Fig. 7 were carried out to measure endocytosis of CD22 in BJAB and Daudi cells, and transfected CD22 or Siglec-F in CHO cells. Western blots were developed with αCD22 (H221) for all B cell lines, and with αV5 for the CHO cell lines.

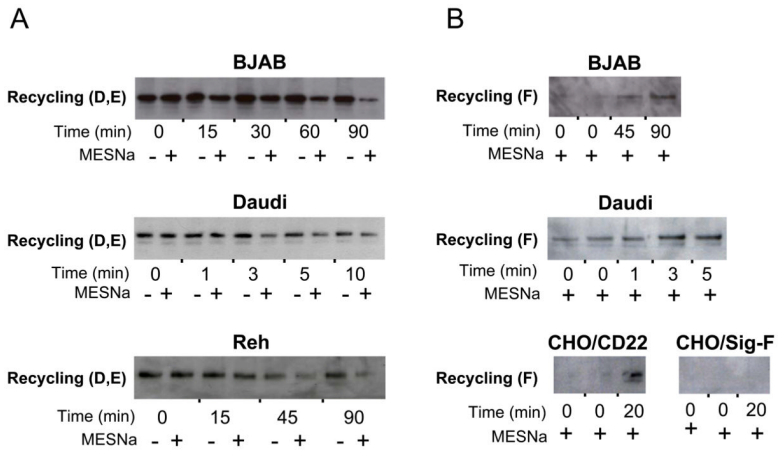

Figure 9. Recycling of biotinylated CD22

Shown are recycling experiments under two protocols. A. Recycling detected by increased sensitivity of endocytosed biotinylated-CD22 to MESNa treatment over time. This assay was conducted on BJAB, Daudi, and Reh cells as illustrated by Steps C-E in Fig. 7. The difference in intensity between MESNa treated and untreated samples after recycling indicates the extent of recycling. B. Recycling detected by capture of recycled biotinylated CD22 with streptavidin magnetic beads prior to lysis. BJAB, Daudi, and transfected CD22 or Siglec-F in CHO cells were tested as illustrated in Steps C,D, and F from Fig. 7. Western blots were developed with αCD22 for all B cell lines, and with αV5 for the CHO cell lines.

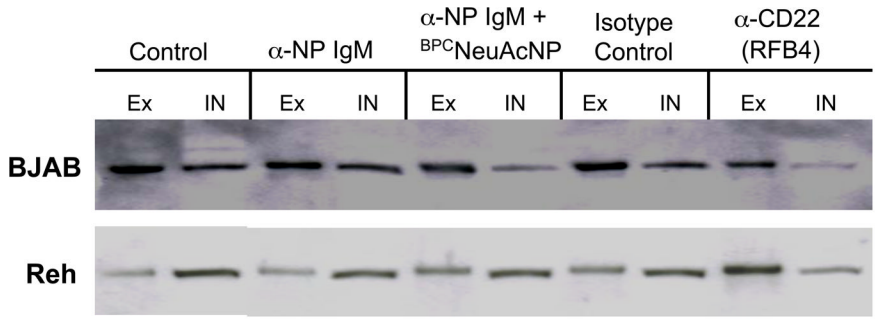

Figure 10. Redistribution of CD22 to the cell surface by αCD22 but not by CD22 ligand-based cargo

BJAB or Reh cells were incubated alone or in the presence of either αCD22, isotype control, or αNP (+/− ^{BPC}NeuAc-NP) at 37 °C. Following incubation, cells were biotinylated at 4 °C and lysed. Surface CD22 was isolated with streptavidin beads, while the supernatant was saved to analyze non-biotinylated, intracellular CD22. Volumes applied from bead capture (Ex; external CD22) or lysis supernatant (In; internal CD22) were normalized prior to western blot analysis to represent an equivalent aliquot of the total sample.